

Robust Segmentation for Low Quality Cell Images from Blood and Bone Marrow

Chen Pan, Yi Fang, Xiang-guo Yan, and Chong-xun Zheng

Abstract: Biomedical image is often complex. An applied image analysis system should deal with the images which are of quite low quality and are challenging to segment. This paper presents a framework for color cell image segmentation by learning and classification online. It is a robust two-stage scheme using kernel method and watershed transform. In first stage, a two-class SVM is employed to discriminate the pixels of object from background; where the SVM is trained on the data which has been analyzed using the mean shift procedure. A real-time training strategy is also developed for SVM. In second stage, as the post-processing, local watershed transform is used to separate clustering cells. Comparison with the SSF (Scale space filter) and classical watershed-based algorithm (those are often employed for cell image segmentation) is given. Experimental results demonstrate that the new method is more accurate and robust than compared methods.

Keywords: Blood and bone marrow, image segmentation, mean shift, SVM, watershed transform.

1. INTRODUCTION

The analysis of blood and bone marrow slides is a powerful diagnostic tool for the detection of leukemia. In order to determine the type of leukemia, the different lineages and maturity levels of white blood cells, which come from peripheral blood or bone marrow, need be recognized and counted. Whereas systems for the analysis of stained blood cells (either using flow cytometric methods or panoptically stained blood slides) that yield a pre-classification are commercially available, the analysis of bone marrow smears is much more difficult [1].

The most important step of automatic analysis is segmentation, which differentiates meaningful objects from the background. This step is crucial since the segmentation result is the basis of subsequent analyses. It's also a difficult and challenging problem due to the complex nature of the cells, low resolution and

complex scenes in the microscopic images. For examples, in one hand, cells often overlap each other and have different sizes and shapes. In the other hand, the color and contrast between the cell and the background often vary according to the inconsistent staining technique, thickness of smear and illumination. Although standardization is a useful means to avoid great change of feature of cell in image acquisition, a robust segmentation approach that can cope with the effects of variation automatically is remarkable in the computer vision. It brings benefits to an applied image analysis system undoubtedly.

One natural way for color image segmentation is to do pixels clustering or classification in color space. Unsupervised and supervised schemes [2], such as c-means, neural network et al., have been widely used for this purpose many years. But there are many disadvantages should be noticed in implementation. Generally, the biggest problem of an unsupervised clustering scheme is how to determine the number of clusters, which is known as cluster validity. And as for a color image, the selection of color space is quite critical. The supervised scheme needs training. The training set and initialization may affect the results, and overtraining should be avoided. So a supervised clustering/classification algorithm with good generalization property is most appealing.

Our basic idea is to solve the segmentation in a nonlinear feature space obtained by kernel methods in order to overcome the nonlinearity of data distribution and the shift/offset of color.

Support vector machine is a popular scheme of the

Manuscript received May 19, 2005; revised January 10, 2006; accepted June 19, 2006. Recommended by Editorial Board member Sun Kook Yoo under the direction of Editor Keum-Shik Hong. This work was finished in Key Laboratory of Biomedical Information Engineering of Education Ministry, Xi'an Jiaotong University. The authors thank anonymous reviewers for some helpful comments.

Chen Pan is with the School of Mathematics & Computer Engineering, Ninxia University, Yingchuan, P. R. China (e-mails: panchen@mailst.xjtu.edu.cn, pc916@nxu.edu.cn).

Yi Fang, Xiang-guo Yan, and Chong-xun Zheng are with the Institute of Biomedical Engineering, Xi'an Jiaotong University, Xi'an, P. R. China (e-mails: bmenfangyi@hotmail.com, {xgyan, cxzheng}@mail.xjtu.edu.cn).

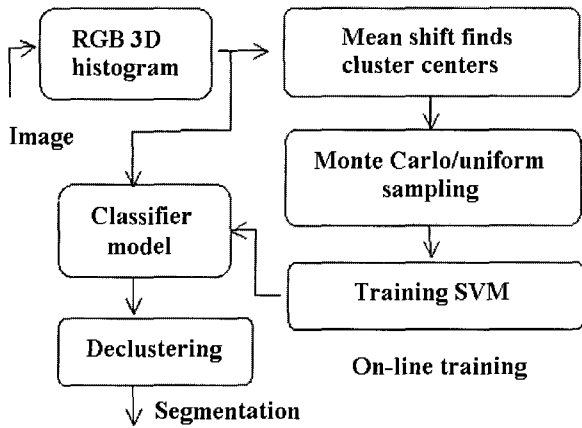


Fig. 1. The framework of the image segmentation system.

kernel method. Recently, it has been implemented in segmentation of MRI, ultrasonic and hyperspectral remote sensing images [3,4]. It exhibits desirable properties such as independence on the feature dimensionality and good generalization performance.

In our study, segmentation of cell image is considered as a two-class classification problem, a two-class SVM with RBF kernel is proposed to classify image pixels into interest and non-interest regions. However, two problems appear in the work. Since SVM is a supervised learning approach, one problem is the training samples should be obtained beforehand. The other is that suffering from enormous computation in the case of large-scale pixel samples, SVM is not virtually practical.

In this paper, combining with the prior knowledge of white blood cell, a sample pre-selecting technique based on mean shift algorithm [5] and uniform/Monte Carlo sampling is utilized to sharply reduce the training set, while retaining the most valuable distribution information. So that training a SVM model can be completed in real time in our work. We present a framework to segment cell image by learning and classification on-line (see Fig. 1). Through pixels-classification, object pixels can be extracted, and next a post-processing separates clustering cells. A detail description is followed in the next sections.

2. PIXEL CLASSIFICATION BY SVM

2.1. Using mean-shift to overcome the variation of color and get training samples for SVM

Mean shift, a simple nonparametric technique for estimation of the density gradient, is used in our work to find the local clustering centers (modes) in histogram. It is an iterative procedure to find fixed point by an initial search window. See reference [5] for detail. The mean shift vector can be described as:

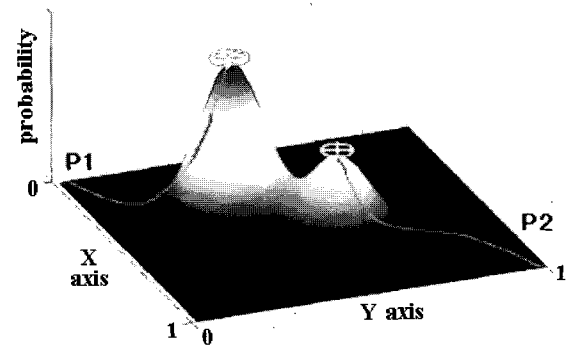


Fig. 2. Two search windows (P1 and P2) find their modes automatically by mean-shift, respectively.

$$m_K(\mathbf{x}) = \frac{\sum_{i=1}^n \mathbf{x}_i k_1\left(\left\|\frac{\mathbf{x}-\mathbf{x}_i}{h}\right\|^2\right)}{\sum_{i=1}^n k_1\left(\left\|\frac{\mathbf{x}-\mathbf{x}_i}{h}\right\|^2\right)} - \mathbf{x}, \quad (1)$$

where $k_1(s)$ is a kernel function represents a search window, h is the bandwidth of k_1 , \mathbf{x} is the center vector of the current window and \mathbf{x}_i is the i th point in this window. The shifts of the window are always in the direction of the probability density maximum (mode). At the mode, the mean shift is close to zero. This property can be exploited in a simple, adaptive steepest ascent algorithm. It is mentioned in [5] that the formula (1) can converge at zero with a certain number of iterations (see Fig. 2). In summary, we can describe mean shift algorithm as below:

- ① Select a proper kernel function as the search window.
- ② Choose the bandwidth of the window and locate the initial window.
- ③ Compute the mean shift vector and translate the search window by that amount.
- ④ Repeat till convergence.

Comaniciu and David [5,6] had presented a mean-shift based approach for segmentation of nucleus of cell. It is robust to those images with different color, sharpness, contrast, noise level and size. However, mean-shift is a low-level technique for feature space analysis. The bandwidth of the kernel should be adjusted carefully, by which the user controls the resolution of the analysis. Mean-shift clustering also suffers from the problem of cluster validity and needs a properly color space. The other shortage is that the features with lesser support in the feature space may not be detected in spite of being salient for the task to be executed [5].

Due to above reasons, mean-shift based scheme has

not enough power to distinguish the different objects with similar color. It is only suitable to analysis the modes with enough difference each other. Since the cytoplasm varies according to the class of cells, its color may only have subtle visible difference to other objects (such as non-cell regions) in many cases. The segmentation of cytoplasm often failed in Comaniciu's approach.

In our study, blood and bone marrow smears are conventionally prepared with Wright-Giemsa stain. In RGB histogram, we can observe the colors corresponding to the regions of nucleus, non-cell and mature erythrocytes are always stained stably, so the corresponding clustering modes are distinct, respectively. Although color shift often occurs in different cell images, the topology of their three clusters is not change a lot. Obviously, if we find their clustering centers adaptively, the color shift of image could be conquered.

Generally, the color of the non-cell regions always nears the brightest point and that of nucleus nears the darkest point in RGB color space. The mature erythrocyte also shows its color properties in limited range different from others. According to above prior knowledge, our new method only concerns three obvious clustering modes. Those modes can be found easily by mean shift from some fixed initial locations. In practice, the initial locations of the search windows corresponding to nucleus and non-cell regions could be fixed to darkest and brightest point in 3D histogram (see p1 and p2 in Fig. 3(d), respectively). The initial windows corresponding to mature erythrocytes could be set experientially or specified manually (see p3 in Fig. 3(d)).

When three clustering modes have been found, the corresponding vectors near the modes (within radius $r \leq h/2$) are mapped back to image domain. Next, the key step is that the regions of nucleus are dilated suitably in order to get a part of cytoplasm pixels. In this way, the prior knowledge about spatial information of blood cells is also taken account into the scheme. Thus, four different regions form candidates of training set for SVM. Generally, cytoplasm and nucleus pixels of white cells are marked with I^+ , and mature erythrocyte and non-cell region pixels are marked with I^- . To avoid uncertainty, we set $I^+ \cap I^- = \Phi$ (empty set). Let the set of candidates (\mathbf{x}_i, l_i) , $\mathbf{x}_i \in I^+ \cup I^-$, $l_i = \begin{cases} +1, & \text{if } \mathbf{x}_i \in I^+ \\ -1, & \text{if } \mathbf{x}_i \in I^- \end{cases}$. $\mathbf{x}_i = (R, G, B)^T$, where (R, G, B) is the color value of pixel.

In order to insure mean-shift converges to correct mode to get training samples, the location of the initial window is a key parameter. Fortunately, in

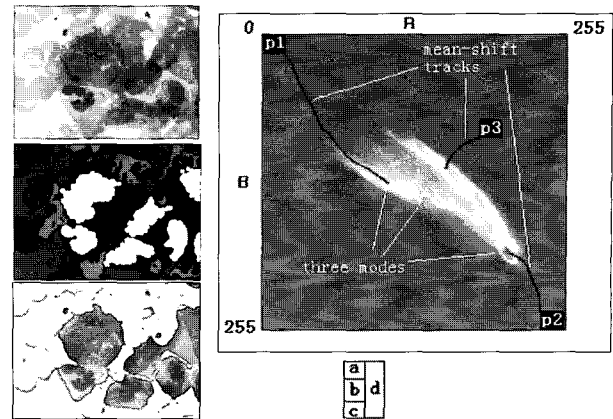


Fig. 3. (a) Original image (760*570 pixels). (b) The candidates include four types of pixels labeled with different gray level, in which pixels of nucleated cells (nucleus and some cytoplasm) labeled with white. (c) The segmentation result classified by SVM trained with all candidate pixels. (d) Three clustering centers (modes) and corresponding mean shift tracks are illustrated in RB color plane.

mean shift algorithm, the corresponding mode can tolerate the initial window in everywhere of its attraction field. This tolerated margin leads to capability of robust. Actually, among three initial windows, only the initial location of mature erythrocyte gives large effect to the result of segmentation if the great change of color occurs.

Our method is similar to the Comaniciu's scheme, but focuses on seeking three meaningful modes rather than analysis all modes of the color space using hundreds mean-shifts. This strategy brings two benefits: (1) The result of mode seeking is not sensitive to the bandwidth of the kernel; (2) Mode seeking can be completed in real time.

2.2. Fast training of SVM

Training of SVM involves optimization of a convex cost function, choice of the kernel function and adjusting few parameters. Various algorithms have been proposed to speed up the optimization of convex cost function and tuning multiple parameters for SVM automatically [7]. Due to prior knowledge of the data is seldom considered, however, these algorithms cannot run fast in implementation, especially in training.

SVM implements a classification strategy that exploits a margin-based "geometrical" criterion rather than a purely "statistical" criterion. It does not estimate the statistical distributions of classes for classification, while defines the classification model by exploiting the concept of margin maximization. There are two types of margin in SVM [8], hard

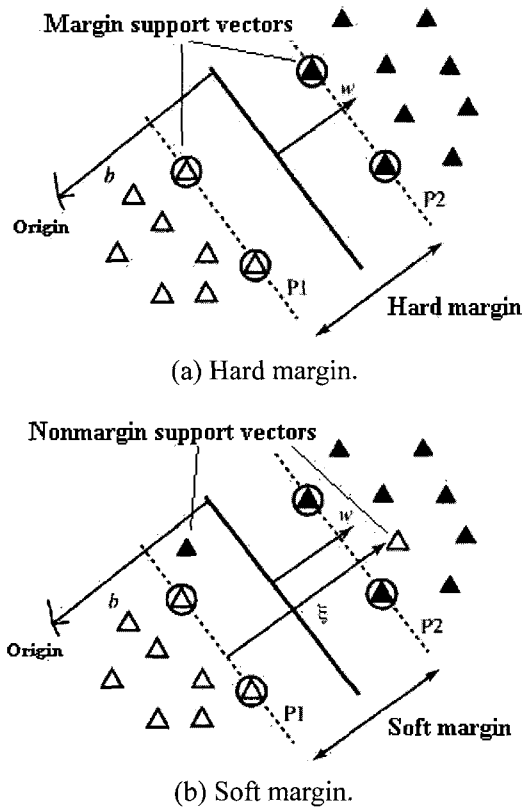


Fig. 4. Illustration of SVM.

margin and soft margin corresponding to object function (2) and (3) respectively.

$$\min \frac{1}{2} \|\mathbf{w}\|^2, \quad (2)$$

$$\min \frac{1}{2} \|\mathbf{w}\|^2 + C \sum_i^n \xi_i. \quad (3)$$

Hard margin classifier works well in no-noise cases, but fails in the noisy data due to overfitting [7,8]. Soft margin classifier may achieve much better generalization results by relaxing the hard margin and ignoring the noisy data. However, two kinds of support vectors (SVs) coexist in the soft margin case: (1) margin support vectors that lie on the hyperplane margin and (2) nonmargin support vectors that fall on the “wrong” side of this margin [9] (see Fig. 4). The latter SVs are regarded as noisy samples that should be ignored. It well known that reducing the computational cost of the SVM is equivalent to decreasing the number of the nonmargin SVs [8,9]. So removing noisy samples from the training set may benefit to training. From the view of the time cost, training an optimal soft margin needs to adjust more parameters and cross-validation often be used, those make the training speed slowly as the training set is large.

As mentioned in Subsection 2.1, the mean shift

procedures find candidates of training set in 3D histogram. Intuitively, histogram is a statistical space that provides excellent tolerance to a noise level [5]. It's well known that noisy data is at least one of the following types: (a) overlapping class probability distributions, (b) outliers and (c) mislabeled patterns [10]. Such noisy data can be easily restrained in histogram by higher statistical value. Because the candidates come from clustering centers (modes), they almost are pure samples without noise. So the classifier model could be adopted hard margin SVM or soft margin SVM with fixed C .

Since SVM only concerns for a classifier is the distribution of training set rather than the size of it, such property would be helpful to reducing the size of training set. Statistics theory has revealed that, through uniform (or Monte Carlo) sampling, a subset could be produced to represent the entire data set approximately while retaining the distribution of data effectively.

The important steps in this subsection can be firstly summarized as follows:

- ① Sample N pixels from I^+ and I^- regions. There are $N/4$ pixels sampled respectively from four regions (cytoplasm, nucleus, mature erythrocyte and non-cell region) to keep the balance of the size of training subset.
- ② Train a SVM online (by SMO method) using the reduced training set, RBF kernel. Then generate a classifier model.
- ③ Use above model to classify the image pixels which are represented by $(R, G, B)^T$.

In order to illustrate how to resample the training data, two important relation curves are investigated and shown in Fig. 5. In which classification accuracy (CA) and training time is regard as indicates of performance of SVM classifier. SVM is trained by the data sampled uniformly from the candidates. The candidates come from Fig. 3(b) in this paper.

The classification accuracy (CA) is defined as follows:

$$CA = 1 - \frac{|N_1 - N_2|}{N_1}, \quad (4)$$

where N_2 is the area of all nucleated cells classified by SVM that trained with small samples, and N_1 is the area of the corresponding cell regions drawn the outline by expert manually.

N indicates uniform sampling N pixels from the candidates. In Fig. 5, since the range of N is large, it is showed with common logarithm of N .

Fig. 5(a) shows CA is not sensitive to the increase of N . The CA- N curve is close to the response of a step function. The inflexion appears early when N is

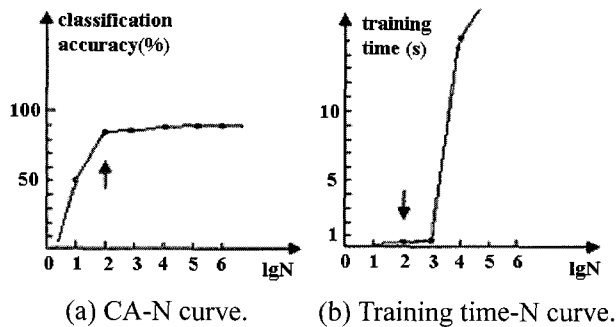


Fig. 5. Relation curves.

very small, such as $N=100$ in this paper. Fig. 5(b) indicates the larger N corresponding to longer training time. An experiential optimal N could be set 1000. In this point, not only CA could be preserved, but also the training time is very short. Such results can also be obtained by Monte Carlo sampling.

In our example (Fig. 3(a) and (b)), the original image (760×570) contains over 430,000 pixels and the whole candidates more than 200,000 pixels, while the training set is not more than 1,000. The ratio between training set and whole candidates is less than 0.5%. The ratio between training set and test data is less than 0.23%. Thus, the reduced training set can be regarded as an efficient representation of whole data. Since the size of the training set does not exceed N pixels, training a SVM online by SMO method is very fast. In this example, the training time is always less than 0.4 second using C program in a personal computer.

3. LOCAL WATERSHED TRANSFORM FOR DECLUSTERING

After pixels-classification by SVM, the white cells can be extracted from background. In bone marrow smears, however, large clusters of white cells exist which have to be declustered [1]. Morphological techniques are attracted for declustering [1,11]. In which marker-controlled watershed transform is popular because it can get more accurate results than others. Yet, some shortages are appeared in implementation. One is that method works well in uniform area, but fails in high gradient region. The other is that method is a seed-dependent. Different location of the seed may lead to different results when the area of the seed is small. So maximum the regions of the seed will benefit to our task.

In this section, we propose an improvement algorithm that peels off the seed of individual cells from the clustering by a distance-transform and builds the borderline of cells by the watershed transform. Because the watershed used here is limited to the local regions segmented by SVM, without involving the mature erythrocyte and non-cell regions, it is defined as "local watershed transform" in this paper.

Our declustering scheme is composed with two similar steps sequentially, which are described as follows:

The first step separates the clustering cells that are overlapping in cytoplasm where the pixels of deep stained don't join to the distance-transform. That is to say, the seed regions will include all pixels of nucleus and most deep stained grains in the cytoplasm, which are not eroded in distance-transform, until the most clustering cells are divided. Then the borderlines between the divided cells are built by the local watershed-transform. Next the individual cells will be selected from the clustering.

The second step aims to separate the rest clustering cells that are mostly overlap in nucleus. This step differs from the former in which the distance-transform involves every pixel.

In each step, the distance transform is controlled adaptively by a criterion of geometrical features of individual cell. Once a part connected pixels is divided from the clustering by erosion procedure, the geometrical features of it such as perimeter and area are measured, and then the compactness of it is computed by the formula: $perimeter^2 / (4\pi \cdot area)$.

When the parameter-pair (area-compactness) falls in certain range of the parameter coordinates, such as satisfied region that is shown in Fig. 6, the corresponding pixels region will be removed from the distance-transform and regarded as the seed for building the borderlines by the watershed transform.

Fig. 6 is an experiential criterion in terms of white cell zoom in 1,000 times. This criterion also be used to select individual cells. It shows if the peeled off region is a part of an individual white blood cell, its compactness should be close to 1.0 when its area is larger, whereas relaxed a little when area is smaller.

By doing so, the seed regions prepared for the watershed transform which are almost maximum. Due

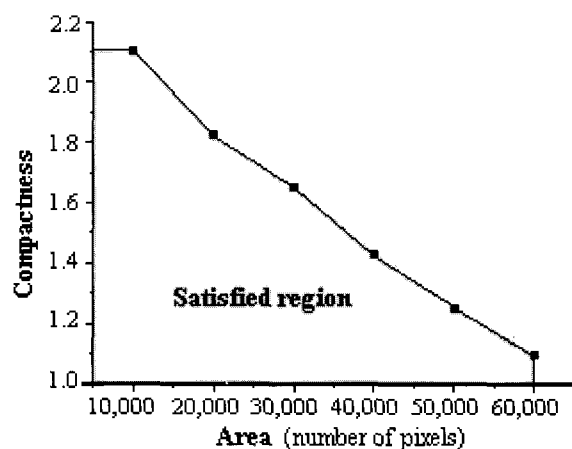


Fig. 6. An experiential criterion of geometrical features of individual white blood cell zoom in 1000 times.

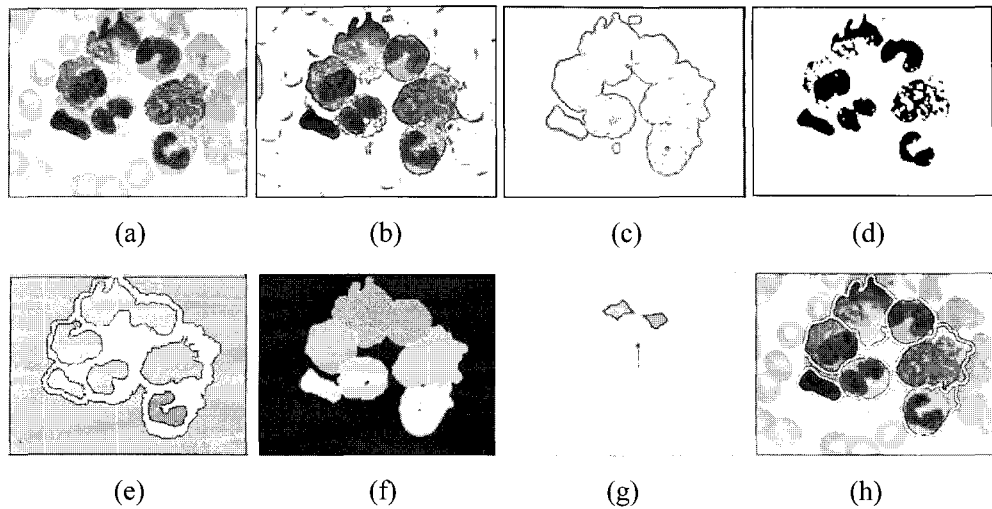


Fig. 7. (a) original image, (b) the object region resulted from pixels classification, (c) the gradient image of object region, (d) deep stained pixel region (obtained by Otsu's method), (e) the maximum seed regions include deep stained pixels, (f) the reconstructed borderlines with the maximum seeds, (g) the seed regions prepared to solve the nucleus overlap, (h) final results of declustering.

to the region in which the borderline need be rebuilt is very small, the new declustering method is much faster than the traditional watershed method.

Obviously, such sequential processing can reduce the difficulty of declustering. These new improvements could greatly enhance the segmentation accuracy. The new method can cope with complex case such as a multi-nuclear cell and granularity of the cytoplasm (see Fig. 7).

4. EXPERIMENTAL RESULTS

More than 200 images (760*570) and 693 white blood cells (from 20 slides) had been tested in our study. These images acquired from different devices with various staining and illumination, and the most of them with low resolution (low quality).

Two other methods such as alone watershed and SSF (scale-space filter) algorithm [12] are compared with our method. An expert locates the initial markers (seeds) manually for alone watershed. The color space of SSF is HSV.

Since the high correlation coexists among R, G and B components, unsupervised method hardly evaluates the similarity of two colors in RGB space. The nonlinear transformation of color space, which can get rid of the correlation of above components, may bring robust performance to image segmentation [2]. However, SVM has inherent capability of nonlinear mapping that can realize same goal. So RGB color space representation of the color images may be more suitable than any other spaces for SVM.

All the three methods use the same post-processing for declustering. The precision of segmentation is defined as follows:

$$P_f = \frac{|R_f - S_f|}{R_f} \times 100\%, \quad (5)$$

where S_f is the area of an individual cell obtained automatically, and R_f is the area of the corresponding cell drawn the outline by expert manually. The segmentation results are shown in Table 1.

Table 1 shows when the P_f is less than 20%, almost double higher segmentation accuracy of our method than the alone watershed algorithm, and fourfold higher than the SSF.

Table 1. The number of segmented cells.

P_f	5~10%	11~20%	21~30%	>30%
Watershed	77(11%)	233(34%)	270(39%)	113(16%)
SSF	51(7%)	89(13%)	271(39%)	282(41%)
SVM based	248(36%)	369(53%)	47(7%)	29(4%)

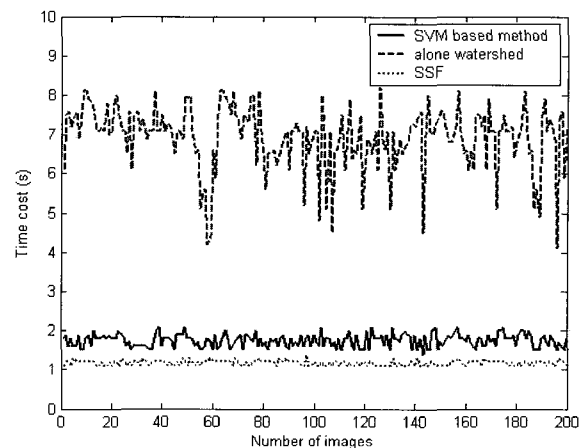


Fig. 8. Comparison in time cost.

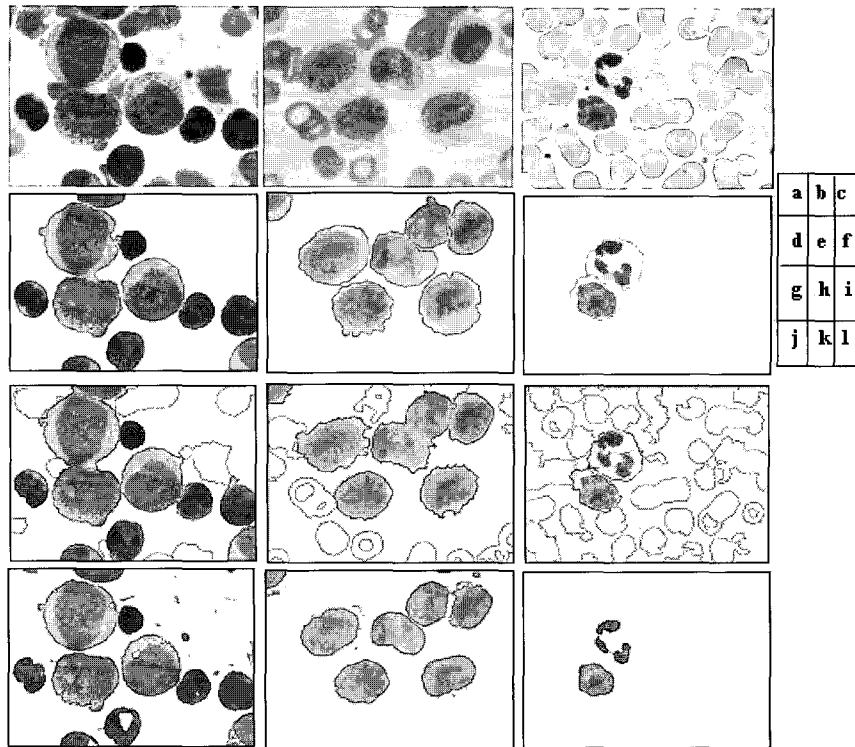


Fig. 9. Comparison of the generalization performance of image segmentation. The first row: three original images, (a) and (b) come from bone marrow, and (c) from blood. The second row (d, e, f): segmentation results by our method. The third row (g, h, i): segmentation results by alone watershed algorithm. The fourth row (j, k, l): segmentation results by SSF method.

The time cost (apart from the post-processing) also compared and result is shown in Fig. 8. That of our method is often less than 2 seconds in this paper. It is superior to alone watershed, close to the SSF.

The different typical cell images with varied source, preparation and lighting are showed in Fig. 9(a), (b) and (c), respectively. The comparison of the generalization performance of three mentioned methods are shown in rest subfigures. Firstly, all the three methods segment Fig. 9(a), in which the parameters of them are optimal selected respectively, so that the segmentation results look like similar (Fig. 9(d), (g) and (j)). However, when different images come in, our method still gets satisfied results (Fig. 9(e) and (f)), but the others cannot do so. Some pixels of cytoplasm are lost near the edge of cells in Fig. 9(h) and (k), and oversegmentation appears in Fig. 9(i) and (l). Since the watershed transform need gradient information and SSF is a thresholding approach actually, the bad generalization performance inherits from their shortages. From the view of the examples, a pure watershed algorithm is easy to be disturbed by an unideal gradient and a threshold is often too coarse to distinguish similar color.

The robust performance of our method is derived from the framework by a learning on-line. Due to excellent performance inherited from the mean-shift and SVM, there are three outstanding characteristics

of the new method: (1) It is an unsupervised learning and classification procedure for image segmentation, so it is not sensitive to the offset of color; (2) The parameters could be universal to same type images, since their histograms are similar each other; (3) The algorithm is fully automatic. Only a key parameter should be adjusted, which is the initial location of mature erythrocyte, if the color of cell image had great change compare with that of the formers.

5. CONCLUSIONS

An applied framework based on learning-on-line strategy for segmentation of nucleated cells from blood and bone marrow images was presented. The contribution of this paper could be summarized into three points: ① We firstly combined SVM with mean shift to solve real computer vision problem; ② A real time training scheme for SVM applied in large scale problems was proposed; ③ A local-watershed-based algorithm was presented to solve the problem of declustering.

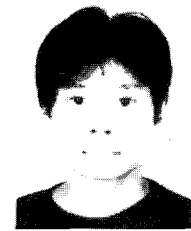
The experimental results demonstrate that the new method is more accurate and robust than some traditional methods such as alone watershed and SSF. It's an effective means to segment color cell images with low quality and complex scenes.

REFERENCES

- [1] H. Hengen, S. Spoor, and M. Pandit, "Analysis of blood and bone marrow smears using digital image processing techniques," *SPIE Medical Imaging*, vol. 4684, pp. 624-635, February 2002.
- [2] H.-D. Cheng, X.-H. Jiang, Y. Sun, and J. Wang, "Color image segmentation: Advances and prospects," *Pattern Recognition*, vol. 34, no. 12, pp. 2259-2281, December 2001.
- [3] C. Kotopoulos and I. Pitas, "Segmentation of ultrasonic images using support vector machines," *Pattern Recognition Letters*, vol. 24, no. 4-5, pp. 715-727, 2003.
- [4] F. Melgani and L. Bruzzone, "Classification of hyperspectral remote sensing images with support vector machines," *IEEE Trans. on Geoscience and Remote Sensing*, vol. 42, no. 8, pp. 1778-1790, 2004.
- [5] D. Comaniciu and P. Meer, "Mean shift: A robust approach toward feature space analysis," *IEEE Trans. on PAMI*, vol. 24, no. 5, pp. 603-619, 2002.
- [6] J. F. David, D. Comaniciu, and P. Meer, "Computer-assisted discrimination among malignant lymphomas and leukemia using immunophenotyping, intelligent image repositories, and telemicroscopy," *IEEE Trans. on Information Technology in Biomedicine*, vol. 4, no. 4, pp. 12-22, 2000.
- [7] C. Campbell, "Algorithmic approaches to training support vector machines: A survey," *Proc. of European Symposium on Artificial Neural Networks*, pp. 27-36, 2000.
- [8] V. Vapnik, *Statistical Learning Theory*, John Willey & Sons, New York, 1998.
- [9] Y.-Q. Zhan and D.-G. Shen, "Design efficient support vector machine for fast classification," *Pattern Recognition*, vol. 38, no. 1, pp. 157-161, 2005.
- [10] G. Ratsch, T. Onoda, and K. R. Muller, "Soft margins for adaBoost," *Machine Learning*, vol. 42, pp. 87-320, 2001.
- [11] N. Malpica, C. O. Solorezano, J. J. Vaquero, and A. Santos, "Applying watershed algorithms to the segmentation of clustered nuclei," *Cytometry*, vol. 28, pp. 289-297, 1997.
- [12] M. J. Carlotto. "Histogram analysis using a scale-space approach," *IEEE Trans. on PAMI*, vol. 9, no. 1, pp. 121-129, 1987.



Chen Pan received the Ph.D. degree in Biomedical Engineering from Xi'an Jiaotong University in 2005. He is currently an Associate Professor of Computer Science at Ningxia University. His research interests include medical image analysis, pattern recognition and machine learning.



Yi Fang is currently a M.S. student in Biomedical Engineering at Xi'an Jiaotong University. He received the B.E. degree in Biomedical Engineering at Xi'an Jiaotong University in 2003. His research interests are mainly focused on the medical image processing.



Xiang-guo Yan is a Professor of Biomedical Engineering at Xi'an Jiaotong University. His research interests primarily are centered with medical signal processing and image processing.



Chong-xun Zheng is a Professor of Biomedical Engineering at Xi'an Jiaotong University. He received the diploma in Electrical Engineering from Xi'an Jiaotong University, China, in 1962. His research interests include biomedical signal processing and applications, image processing, cardiac electrophysiology, neurophysiology, noninvasive bio-signal extracting.